Mechanical properties, wear resistance and surface damage of glasses and $MgAl_2O_4$ spinel ceramic after abrasion and scratch exposure

S. von Helden, J. Malzbender, M. Krüger

Forschungszentrum Jülich GmbH, IEK-2, 52425 Jülich, Germany

Abstract

A transparent spinel ceramic is compared to different types of glasses, including unhardened and hardened material, as well as a polymer in terms of mechanical behavior and optical appearance before and after mechanical exposure. The mechanical behavior of the materials is compared on the basis of depth-sensitive indentation and ring-on-ring bending tests, deriving hardness, elastic modulus, and fracture stress data. The focus of this research is the analysis of specimens after certain exposure times of sand blasting and different loads during scratch tests via weight balance, confocal laser scanning, and optical microscopes to assess wear resistance including surface roughness, mass loss, critical loads, and initial damage. Results are critically discussed in terms of differences in the performance of the diverse materials and the correlation of optical appearance, abrasive behavior, and apparent scratch testing damage. The overall comparison of properties and application relevant to damage resistance indicates that the tested transparent ceramic and the surface hardened Gorilla glass are superior to all other tested variants.

Keywords: Transparent ceramic; Spinel; Glass; Mechanical Properties; Scratch; Abrasion

1. Introduction

Transparent ceramics, particularly spinel, have high potential in their use as transparent armor ceramics and also as protective windows for sensor application as these types of applications require high levels of optical and mechanical performances [1-3]. Previous research has shown that such transparent windows have to combine very good mechanical properties, i.e. hardness, fracture toughness, and wear resistance with high transmission and a suitable refractive index [4-6]. Also, in a potentially aggressive environment these characteristics must be preserved as long as possible to retain the structural integrity and optical transparency. However, the development and optimization of such materials under the conditions of an application relevant environment are mainly based on empirical approaches [4]. Therefore, certain comparative experiments and parameters are needed to classify newly developed and improved materials that can be used as a basis to assess their usability. To that end, the experimental setup is decisive, such as the tip geometry in the case of hardness impressions and scratch tests or the particle type used in an abrasive test [7]. Hence, selection of experiments needs consideration of application relevance and available instrumentation.

For the applications mentioned above, glasses are usually hardened to create a mechanically more resistant surface layer, although sometimes hybrid coatings are used [8]. In this case, an understanding of the mechanical behavior of both the top layer and the bulk material beneath are very important to guarantee an extended life time. For example, it has been proven that tempered glasses are often more sensitive to scratches or abrasion related damages than annealed glasses, leading in case of the former to catastrophic failure once a critical load is exceeded [8]. To avoid such critical issues, it is necessary to follow the regulations of special cleaning methods [9] or even to coat these glasses [10]. In this respect, scratch experiments are considered to be essential in building knowledge of the wear and abrasion mechanism for materials' transport or removal [11-14]. However, for applications that require transparency, such as windows or displays, the optical integrity is even more important than the mechanical

behavior. Here, especially spinel is interesting, because it has significantly higher values of hardness than glasses, a main parameter for impact and wear resistance, and the transparency extends over a broad wavelength range [5].

However, other properties in addition to elastic modulus, hardness, fracture toughness, and scratch resistance are relevant in determining product durability [15]. Indeed, the mechanical durability also depends on the erosive resistance that describes the exposure to flying particles which can lead to material removal [16]. This loading case can be realized experimentally by sandblasting with controlled pressurized air, particle size, duration, angle, and distance to the specimens [17-20]. In this case, for the evaluation of the apparent materials´ behavior, measurements of mass loss, surface roughness, and examination of the optical conditions can be used [16].

The goal of this research is to characterize the basic mechanical properties of the different materials, as well as their scratch and wear resistance, where the chosen polymer material is used as an example of a material that might be used as an alternative to protect optical detection systems. The influence of mechanical exposure on both, mechanical and optical properties, is considered.

2. Materials and experiments

2.1 Materials

The investigated transparent spinel ceramic called Perlucor® is commercially available at CeramTec-Etec GmbH (Lohmar, Germany) with the classical stoichiometry $MgAl_2O_4$. In this comparative study, other common transparent materials, such as Polycarbonate and different hardened and unhardened glasses, i.e. float glass or Borofloat® by Schott, Gorilla® glass 3 by Corning, are studied. In addition to the transparent ceramic, the other materials (commercially supplied by different companies) were purchased and made available by the project partner in

the framework of the ResTraSe project funded by the European Union (see acknowledgements). All specimens had a disc shape with a thickness of 2 mm and a diameter of 25 mm (see **Table 1** for overview). All samples have been delivered in fine polished state and were coplanar with high accuracy. The surface roughness parameters based on ISO 4287:1997, R_a and S_a were both in a range of 0.002-0.01 µm in the initial state measured with the confocal laser scanning microscope mentioned later, and the thickness variation was within the scope of measurement uncertainty ± 0.01 mm of the digital caliper gauge Garant produced by the Hoffmann Group.

2.2 Experimental setup

Density ρ and Poisson´s ratio ν were extracted from the producers´ data sheets [21-27]. Young´s modulus E was measured by an impulse excitation technique with a GrindoSonic® system (Lemens KG, Belgium) based on ASTM E1876-01, where the samples are stimulated mechanically to record the specific natural vibration frequency by a microphone [28]. To determine the hardness H and also to check the Young´s modulus, 25 depth-sensitive micro-indentations with a load each of 10, 100, and 1000 mN were performed, using a Fischer HC100 (Helmut Fischer KG, Sindelfingen) with a Vickers diamond pyramid tip [29, 30] and automatically calculated via the widely used Oliver-Pharr method [31]. The fracture toughness K_{Ic} was calculated from the minimum of 12 optically measured crack lengths induced by a macro-indentation equipment (Micromet Buehler LTD.) at applied loads of 2.94 and 4.9 N, again 25 indents each load, using the following equation for the median crack systems by Anstis et al. [32]:

$$K_{Ic} = 0.016 \left(\frac{E}{H}\right)^{0.5} * \left(\frac{P}{c^{1.5}}\right) \quad (1)$$

where P is the load, E the Young´s modulus, H the hardness, and c the half mean length of the radial cracks from tip to tip. This equation is valid, if the criterion $c > 2a$ is fulfilled, where a is the half diagonal of the impression; otherwise, another crack system has to be used. However,

all four hardened glasses had shorter cracks and did not satisfy the condition $c \geq 2a$ for equation (1) anymore. Therefore, in these cases the equation for a Palmqvist crack geometry was considered following Evans et al. [33]:

$$K_{Ic} = 0.079 \left(\frac{P}{a^{1.5}}\right) * log\left(4.5\ \frac{a}{c}\right) \quad (2)$$

Ring-on-ring bending experiments were performed in an electromechanical testing machine INSTRON 1362 with a ±10 kN load cell from Lebow Corporation, while the displacement of the specimens was quantified with a ceramic extension rod connected to a linear variable differential transformer, Solartron Metrology. During the experiments, the disc shaped samples rested on a fixed supporting ring and were loaded via a loading ring until fracture. Following ASTM C1499-05, the maximum stress at failure was calculated using linear bending theory [34]. A loading rate of 1000 N/min was used with diameters of supporting and loading ring of 18.96 mm and 9.47 mm, respectively. Subsequently, the experimental data were used in a statistical analysis to measure the average fracture stress, as well as the characteristic strength and Weibull modulus by linear regression [35]. Within this distribution, it is possible to estimate an interval, which includes the stress-probability distribution. This confidence interval consists of an upper and lower bound of that limit, with a certain probability (confidence level of for example 95%), the range where the data are included, according to DIN EN 843-5 [36].

For the sandblasting, in a sandblasting machine MHG BNP 210 (MHG Strahlanlagen GmbH, Düsseldorf), a special sample holder was designed. The test method is a novel development with a special sample holder that might be useful for wider industrial use as alternative for currently used testing procedures. The experimental setup is illustrated in **Figure 1**. The holder allows placing the samples always in the same position, with the same distance and an angle of 45° to the beam. It is fixed with magnetic holders to the plate of the sandblasting box. The sand blasting pistol itself is also rigidly fixed to ensure a constant beam alignment. Glass beads, also

produced by MHG, with an average grain diameter of 150-250 µm [37] were used as the grid in pressurized air (2 bar).

After exposure times of 5, 30, 60, 120, and 300 s, the samples were taken out and optically investigated with a reflex camera Nikon D300S in UHD resolution. Before and after the experiments, the specimens were weighed with a precision balance Mettler-Toledo XS205 Dualrange (Mettler-Toledo GmbH, Gießen) with a measuring accuracy of 0.01 mg to calculate the mass loss and additionally analyzed through a 3D confocal laser scanning microscope Olympus LEXT OLS4000 to ascertain the surface roughness through the producers' Olympus software.

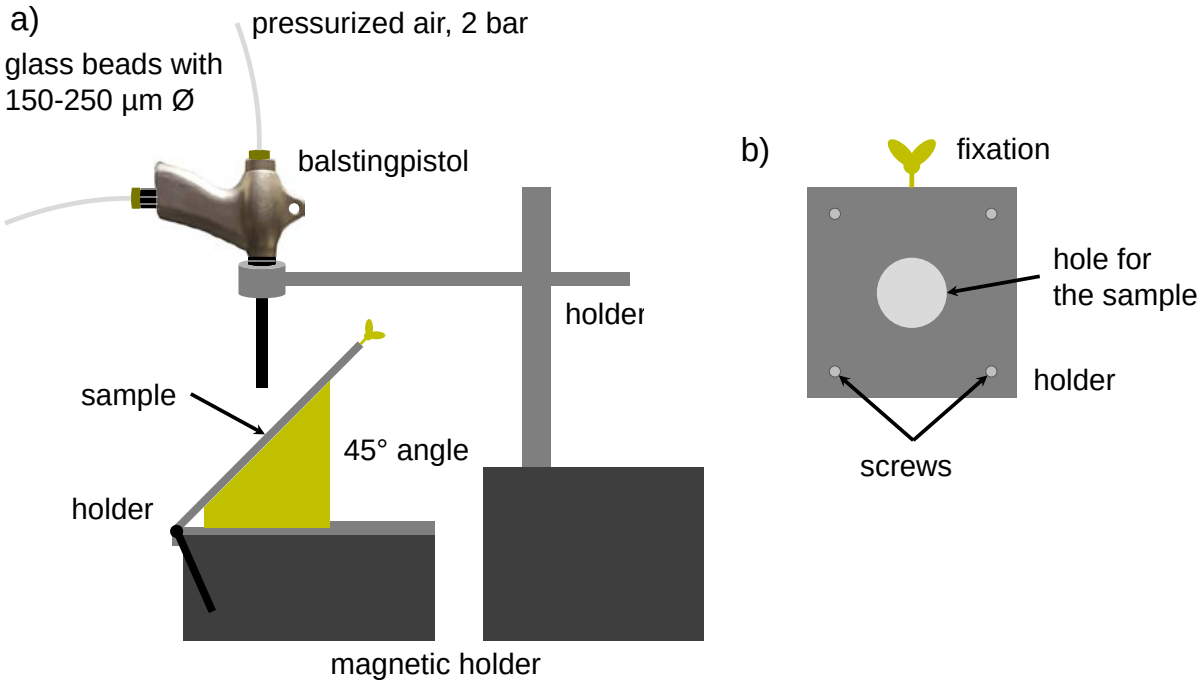

Figure 1: a) Experimental setup for the sandblasting, b) details of the sample holder.

In order to characterize the scratch resistance of the materials, three scratches on each sample were carried out with a sphero-conical diamond tip under a load progressively increasing from 0.03 N up to 5 N using a horizontal displacement rate of 1 mm/min. For these experiments, another depth-sensitive indentation unit was used, a nano-/micro-indenter system CSM (Anton Paar GmbH, Graz, Österreich), which possesses a high-resolution multi-objective microscope

up to 100x magnification, by Nikon. The cone of the penetrator had a 90 degrees angle; the spherical part had a 50 µm radius and was cleaned with ethanol before each test. All tests were carried out on the same day under the same environmental conditions at room temperature, to ensure a constant humidity. The optical analyses were made with a digital microscope, the Keyence VHX-5000, and an objective, the VH-Z 20 UR, RZ with a 20-200x magnification range, directly after the testing to minimize effects related to possible subcritical crack growth / fatigue phenomena.

Table 1: Materials and their properties, *E*, *H* and K_{IC} derived in the current work. ρ and ν from [21-27].

Material	ρ [g cm^{-3}]	ν	E [GPa]	H [GPa]	K_{Ic} [MPa√m]
Perlucor	3.57	0.25	287 ± 6.5	18.9 ± 1.1	2.77 ± 1.25
Polycarbonate	1.2	0.4	7.3 ± 2.4	0.2 ± 0.1	-
NBK-7	2.51	0.206	90.2 ± 0.9	8.5 ± 0.3	0.56 ± 0.08
Float glass	2.5	0.2	75.6 ± 1.4	7.5 ± 0.5	0.67 ± 0.05
Float glass hardened	2.5	0.2	72.6 ± 1.7	8.5 ± 0.1	2.08 ± 0.11
Borofloat	2.2	0.2	78.0 ± 0.2	7.7 ± 0.1	1.15 ± 0.13
Borofloat hardened	2.2	0.2	78.4 ± 0.1	8.2 ± 0.1	2.22 ± 0.08
Gorilla glass	2.39	0.22	71.2 ± 0.5	7.7 ± 0.2	0.95 ± 0.05
Gorilla glass hardened	2.39	0.22	67.2 ± 0.2	9.2 ± 0.3	3.37 ± 0.05
B270	2.55	0.219	75.8 ± 0.3	7.4 ± 0.1	0.56 ± 0.05
B270 hardened	2.55	0.219	80.6 ± 0.5	8.0 ± 0.1	1.78 ± 0.17

3. Results and discussion

3.1 Mechanical properties

The measured mechanical properties, along with some data sheet based physical properties, are listed in **Table 1**. In this table, the elastic modulus was determined via impulse excitation, hardness at 100 mN load and fracture toughness at 4.9 N load via macro-indentation testing. The density and the Poisson´s ratio, as well as the hardness and Young´s modulus, do not vary very much between the different glasses. The polymer exhibits the lowest density, Young´s

modulus, and hardness, and displays plastic deformations without cracks in the indentation test. As such, no fracture toughness value could be derived using the indentation test. Due to its structure, long carbon chains and low density, the polymer reveals a high elasticity and thus only a low hardness.

The transparent ceramic displays the highest density, Young´s modulus, and hardness, and also a very high fracture toughness. In fact, the hardness is 10 GPa higher than the highest hardness of the glasses. Furthermore, especially for the hardened glasses, the measured hardness and fracture toughness depend on the used load (see also more details below and in **Table 2**), as opposed to the Young´s modulus, which remains constant during the depth-sensitive indentation testing and has similar results as the impulse excitation, why it is not discussed further here.

It is known that, for ceramics in particular, hardness decreases with an increasing load, which is termed “indentation size effect”. Glasses, however, should not show such an effect unless they are hardened. **Figure 2** illustrates this behavior for selected materials. The indentation size effect is clearly visible in the ceramic and the hardened gorilla glass also shows an obvious decrease in hardness at the beginning, while the unhardened glass is almost constant. For hardened Borofloat the effect is not so distinct. The tip penetrates the hardened surface area at loads above 10 N, and the indentation causes big chipping and can lead to failure of the hardened glasses as shown in **Figure 3** for two samples. Only lower loads result in a clear and optically measurable imprint.

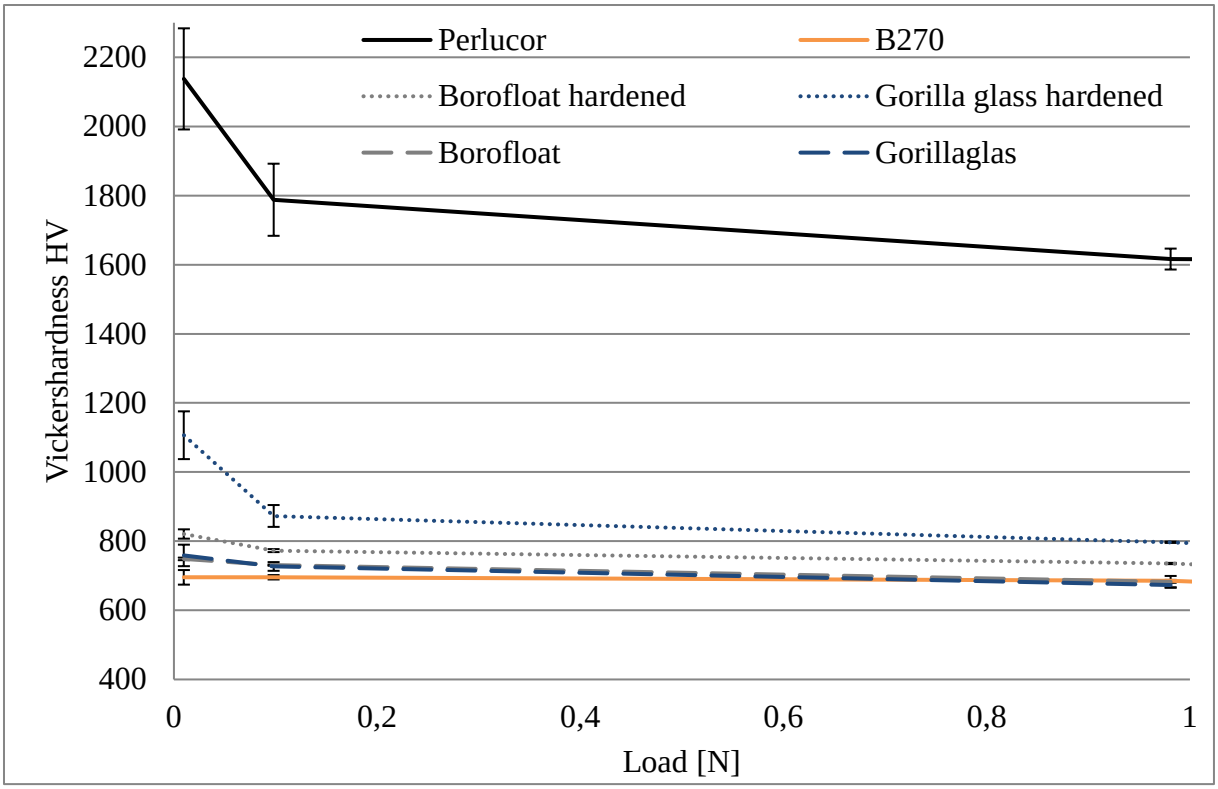

Figure 2: Load dependencies of the Vickers hardness values.

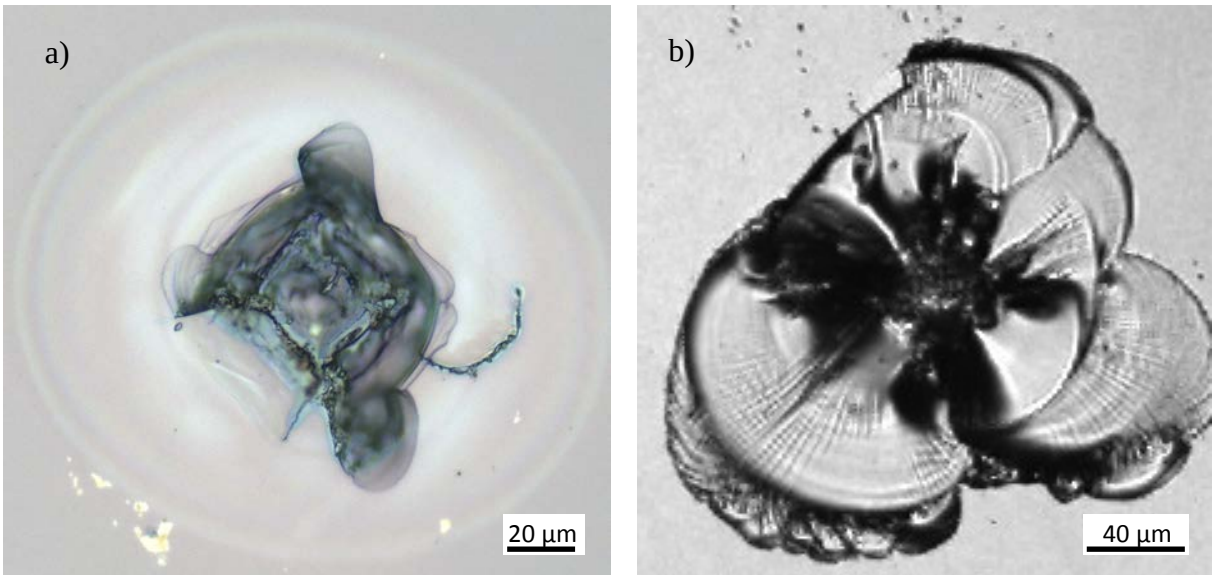

Figure 3: Examples of chipping for a) hardened Borofloat and b) hardened float glass.

There is a big difference in the fracture toughness between the unhardened and hardened versions of the glass types, which cannot only be seen in the size of the indentations, but also in different crack propagations illustrated in **Figure 4**. All hardened glasses possess shorter

cracks, which is why equation (2) and the corresponding Palmqvist crack geometry were used for them.

The results of the measurements are shown in **Table** 2. Although both equations were used for the different materials, the glasses show a constant load independent fracture toughness. In fact, the hardened Gorilla glass reveals the highest fracture toughness and the shortest cracks.

Table 2: Load dependencies of the fracture toughness.

Material	K_{Ic} [MPa√m] at 2.94 N	K_{Ic} [MPa√m] at 4.9 N
Perlucor	2.51 ± 0.6	2.77 ± 1.25
Polycarbonate	-	-
NBK-7	0.52 ± 0.04	0.56 ± 0.08
Float glass	0.59 ± 0.06	0.67 ± 0.05
Float glass hardened	2.07 ± 0.07	2.08 ± 0.11
Borofloat	-	1.15 ± 0.13
Borofloat hardened	2.53 ± 0.25	2.22 ± 0.08
Gorilla glass	0.91 ± 0.03	0.95 ± 0.05
Gorilla glass hardened	3.02 ± 0.12	3.37 ± 0.05
B270	0.64 ± 0.06	0.56 ± 0.05
B270 hardened	1.89 ± 0.12	1.78 ± 0.17

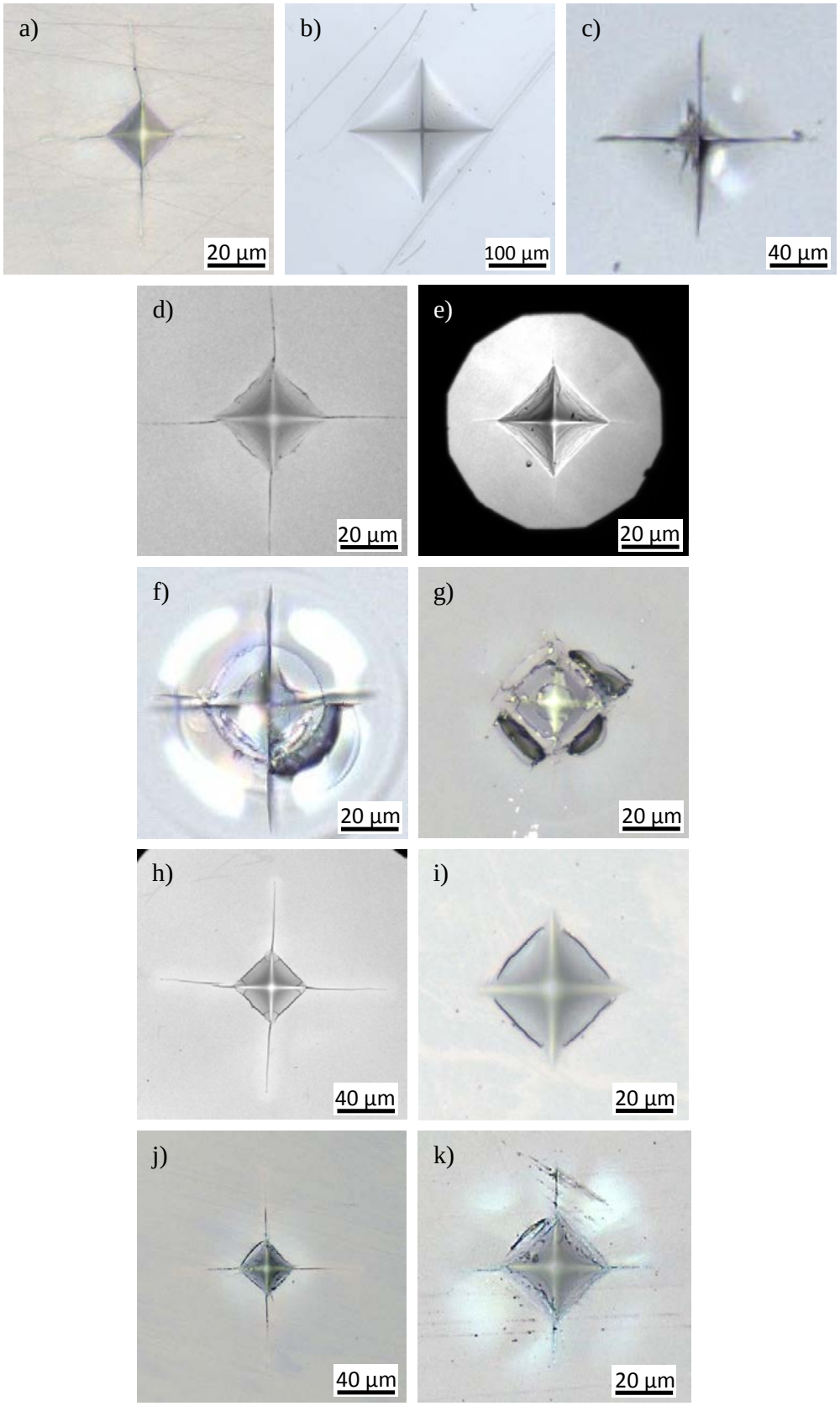

Figure 4: Vickers indentations at 4.9 N for a) Perlucor, b) Polycarbonate, c) N-BK7, d) float glass, e) hardened float glass, f) Borofloat, g) hardened Borofloat, h) Gorilla glass at 9.81 N, i) hardened Gorilla glass at 9.81 N, j) B270, k) hardened B270.

The calculated values for the fracture toughness coincide with values reported by Houérou et al. [38] for float glass, with Li et al. [39] for N-BK 7, with the data sheet for Gorilla glass [22], with Buijs et al. for B270 [40], with Wereszczak et al. [41] for Borofloat and with Tokariev for Perlucor [42].

The average fracture stresses, characteristic fracture strengths σ_0 and the measured Weibull moduli *m* derived on the basis of ring-on-ring tests are presented in **Table 3**. It was not possible to measure values for the polymer, since it was just deformed elastically without fracture. Again, a clear benefit of the chemically hardened glasses can be seen, since the fracture strength is increased by at least a factor of 2.5 as a result of compressive stresses in the surface. For the Gorilla glass, an increase by a factor of more than 6 is obtained, and the hardened one displays by far the highest value among all tested materials. Furthermore, the very high Weibull modulus illustrates the low scatter of the results of the measurements and therefore indicates a strong reliability (stresses are still close to the strength even for lower failure probabilities). In general, the transparent ceramic is comparable with the hardened glasses, except for the hardened Gorilla glass, with a quite higher and hence better value for *m*. On average, the glasses show a lower value for the Weibull modulus, indicating a larger scatter of the failure relevant defects.

Table 3: Results of the bending tests including the confidence intervals (termed lower and upper, respectively).

Material	Av. fracture stress [MPa]	lower σ_0 [MPa]	σ_0 [MPa]	upper σ_0 [MPa]	lower *m* [-]	*m* [-]	upper *m* [-]

Perlucor	294 ± 43	295	312	330	5	8	10
Polycarbonate	-	-	-	-	-	-	-
NBK-7	104 ± 36	88	117	157	1	3	4
Float glass	121 ± 27	113	134	158	2	5	8
Float glass hardened	319 ± 90	280	355	453	2	4	5
Borofloat	71 ± 21	63	79	99	2	4	6
Borofloat hardened	164 ± 35	148	182	225	2	4	6
Gorilla glass	104 ± 23	96	113	135	2	5	8
Gorilla glass hardened	670 ± 47	656	692	731	8	16	24
B270	110 ± 31	98	121	151	2	4	6
B270 hardened	339 ± 39	326	357	392	5	9	14

In conclusion, all mechanical properties can be compared to each other to correlate the differences with respect to the ceramic as the relative reference with all properties normalized to 1 in **Figure 5**. Overall, density and Poisson's ratio have similar values for the different glasses, as well as the hardness and elastic modulus, i.e. high hardness typically is accompanied with high elastic modulus and somehow higher Poisson's ratio and higher density. **Figure 5** indicates that high values for fracture strength are typically coupled with high values for Weibull modulus, except for hardened float glass; note that the Weibull modulus depends on the defect size distribution, which may result in high statistical scatter. Except for both Borofloat types, the fracture toughness increases with increasing fracture strength. For all unhardened glasses, the hardness values follow the fracture strength, but this correlation does not hold for the hardened ones. Only hardened Gorilla glass displays a much higher characteristic fracture strength and Weibull modulus with slightly higher fracture toughness, while the level of hardness is barely half that of the hardness of the ceramic.

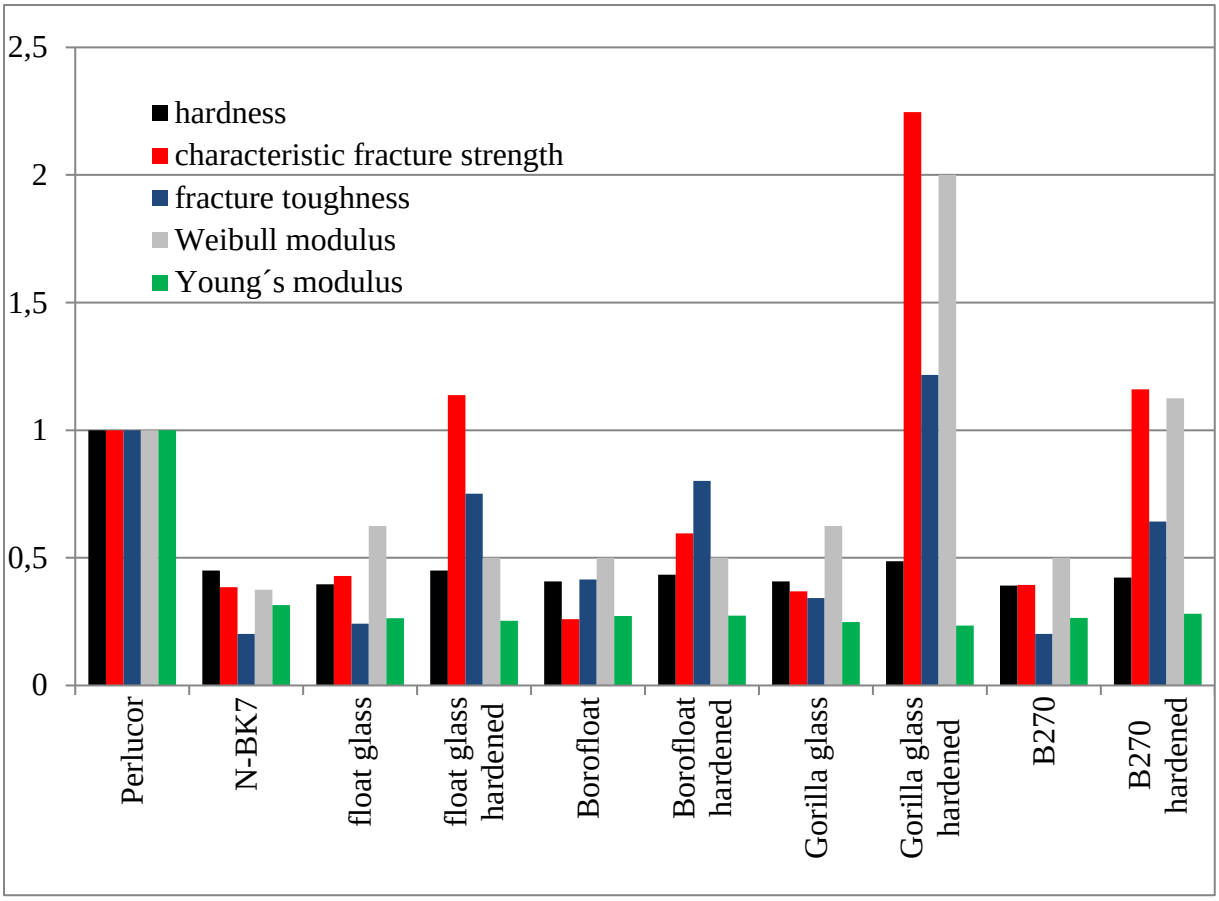

Figure 5: Correlation of mechanical parameters. The ceramic is the reference with all values normalized to 1.

3.2 Sandblasting

The sandblasting beam induces a progressive surface removal due to the 45° impact angle. It can be expected that materials with a higher hardness are more resistant regarding mechanical abrasion. One obvious way to control the application relevant surface changes (deterioration) for a transparent material is an optical verification. Therefore, **Figure 6** gives an overview of photographs of specimens after different exposure times revealing the blurring of the transparency.

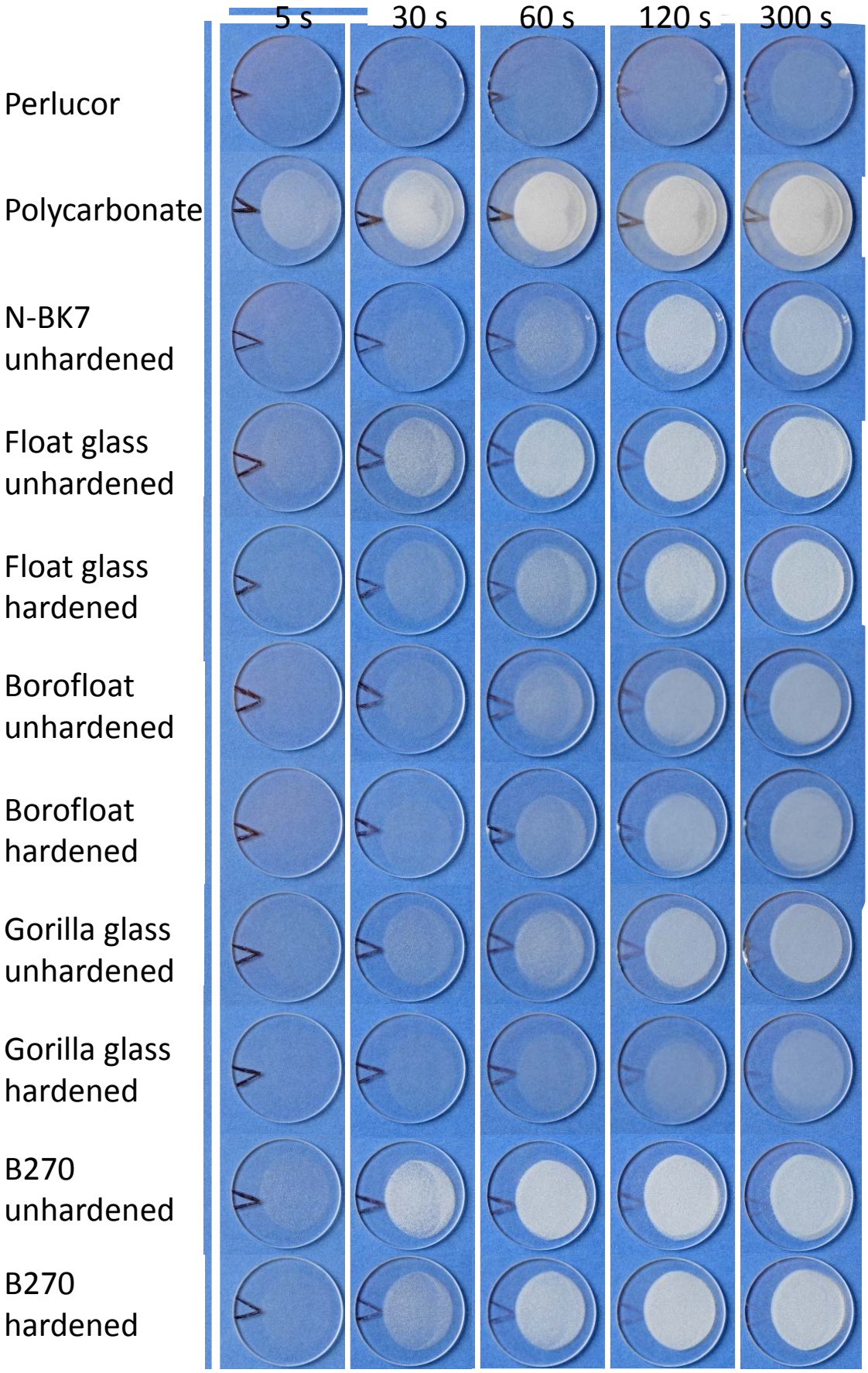

Figure 6: Optical comparison of specimens after different exposure times to sandblasting obtained by reflex camera.

As can be seen in Figure 6, the sandblasting has the highest deteriorating effect on the polymer; an apparent loss in transparency can already be seen just after 5 s exposure time. After 5 minutes it is completely opaque, affecting even some regions of the surface were not directly exposed to the beam. Contrary to this, the spinel ceramic is apparently still transparent with just minor surface degradation even after 5 minutes. The unhardened N-BK7 is representative of the average glass behavior with little mass loss (as will be discussed below), but an obvious blurring; however, it still appears to be usable as a transparent component after 60 seconds. Optically, there seems to be no benefit in hardening of Borofloat, since the visible wear resistance appears to be similar. Overall, it resists wear better than float glass or B270, but not as well as Gorilla glass. The hardened Gorilla glass shows the best abrasion resistance of all glass types, though after 300 s it is no longer transparent. Both float glass and B270 unhardened as well as hardened are short-term prone to abrasion damage, and after 5 minutes, a crater can be seen even with the bare eye for selected materials, as illustrated in **Figure 7**. Additionally, a line scan over the degraded surface area is given, where the relative depth of the crater can be seen. Also, here the ceramic reveals an almost flat line that is devoid of significant surface defects due to the good wear resistance. By contrast, unhardened float glass and B270 display crater depths of 0.2 up to 0.25 mm and therewith a high material removal that distorts the former flat surface. In these regions the light can be refracted, and the transparency is lost.

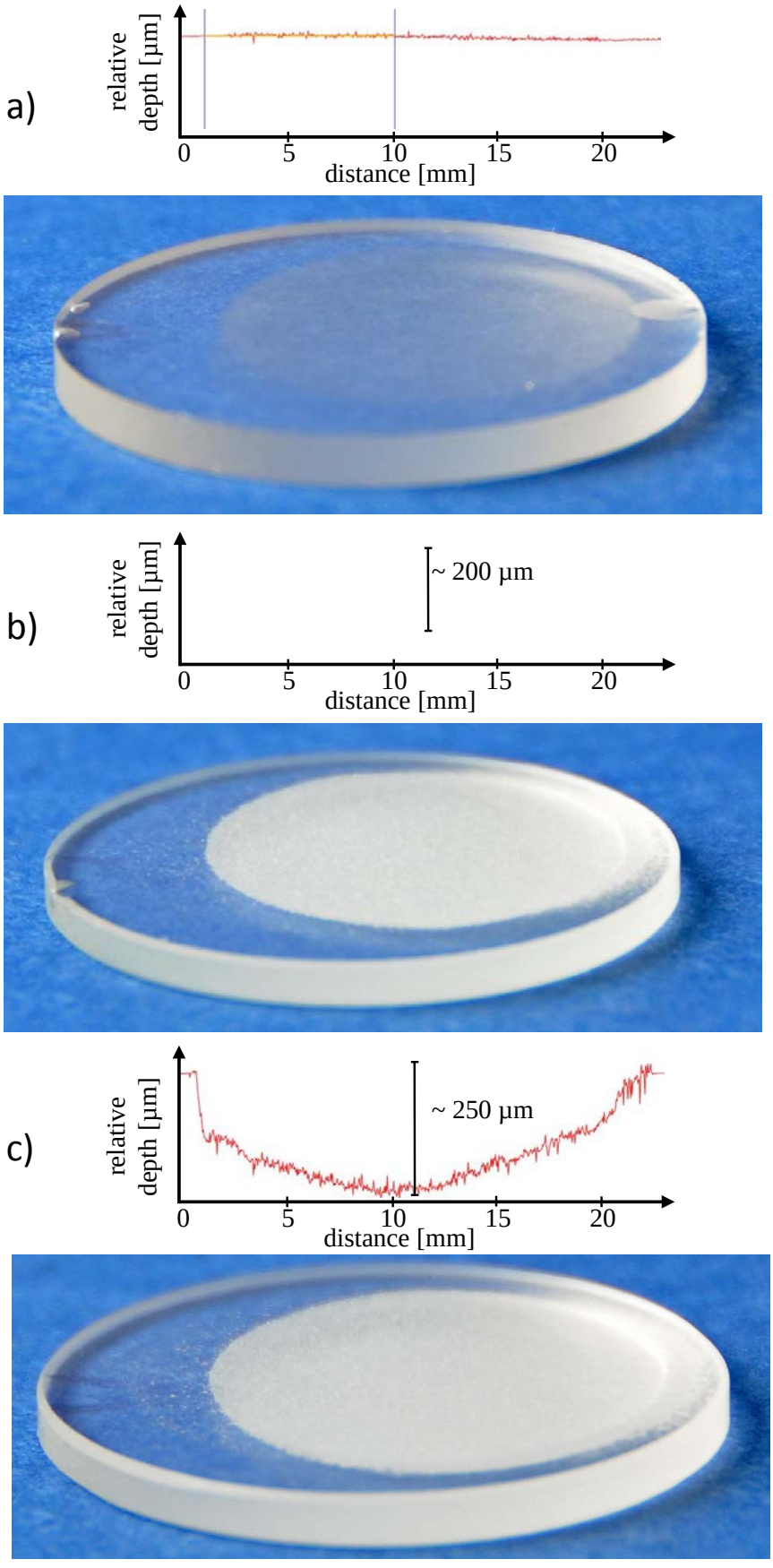

Figure 7: Laterally view on the crater after 5 minutes sandblasting for a) Perlucor, b) unhardened float glass and c) unhardened B270.

In addition, the samples were analyzed via a confocal laser scanning microscope before and after the testing to assess the surface roughness and crater depth. A high precision weight measurement was used to check the mass loss related to abrasion. These results are presented in **Figure 8**. Since all samples were polished, the average surface roughness before testing was similar in the order of R_a = 0.005 µm for the arithmetic average line roughness parameter and S_a = 0.005 µm for the mean arithmetic height (extended surface roughness parameter relating to the area).

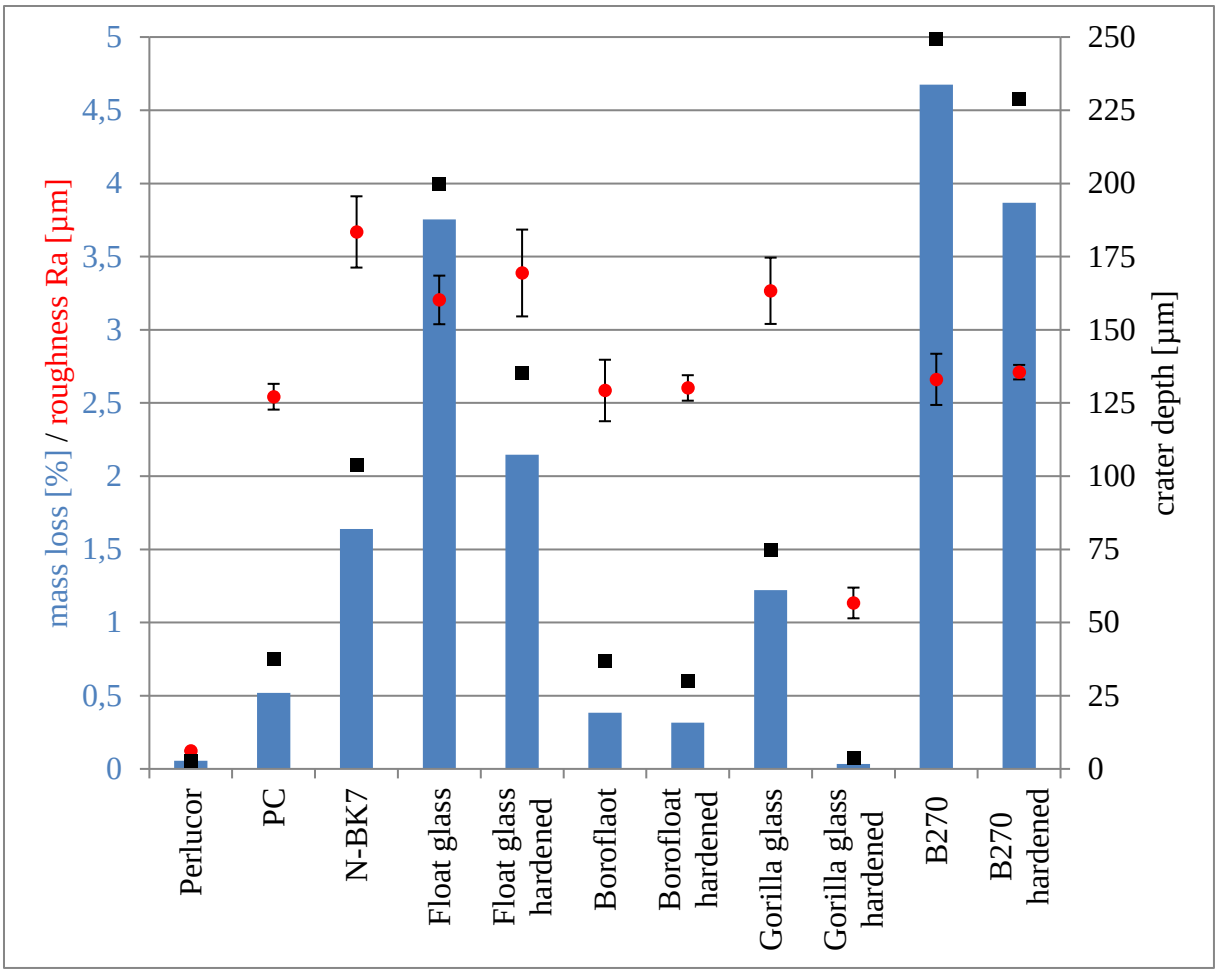

Figure 8: Mass loss, crater depth and roughness after 5 minutes of sandblasting.

As might be expected, the hardened Gorilla glass displays the lowest mass loss, crater depth and roughness out of all the glasses tested in this research. Consistent with the optical analyses, the float glasses and B270 indicate a high mass loss and crater depth as a result of the abrasive

sandblasting. Despite its highly blurred appearance, the polymer does not lose much mass, and because of its very low Young´s modulus, it behaves quite elastic, consuming the impact energy of the glass beads. Interestingly, the mass loss of Borofloat is also very low as well as the formed crater. Again, the spinel ceramic demonstrates the best wear resistance with the lowest roughness and a low mass loss similar to the hardened Gorilla glass. **Table 4** summarizes all results of the sandblasting, including the measured depth of the crater.

Table 4: Results of the sandblasting tests after 5 minutes exposure.

Material	mass loss [%]	mass loss [mg]	R_a [µm]	S_a [µm]	max. crater depth [µm]
Perlucor	0.06	2.0	0.1 ± 0.01	0.1	3
Polycarbonate	0.5	5.8	2.5 ± 0.1	2.2	38
NBK-7	1.6	39.4	3.7 ± 0.4	3.8	104
Float glass	3.8	82.7	3.2 ± 0.4	3.7	200
Float glass hardened	2.1	48.9	3.4 ± 0.3	3.6	135
Borofloat	0.4	8.2	2.6 ± 0.2	2.6	37
Borofloat hardened	0.3	6.8	2.6 ± 0.1	2.8	30
Gorilla glass	1.2	25.6	3.3 ± 0.4	3.6	75
Gorilla glass hardened	0.03	0.7	1.1 ± 0.1	1.1	4
B270	4.7	114.8	2.7 ± 0.2	3.5	253
B270 hardened	3.9	95.6	2.7 ± 0.5	3.8	229

These results indicate that for a good wear resistance, high hardness combined with high fracture toughness is the most important mechanical property. Perlucor and hardened Gorilla glass have the best combination of these two parameters, while the hardness seems to be more relevant for the short term and the fracture toughness for the long term exposure. Both materials show the slightest blurring, correlating with the mechanical properties followed by Borofloat, N-BK7, float glass, B270, and the soft polymer. Except for the special elastic behavior of the polymer, the mass loss and the maximal crater depth give the same ranking. The sandblasting experiment is an application-relevant test that displays the importance of the basic mechanical properties of the investigated materials.

3.3 Scratch behavior

During a scratch experiment, different types of micro-cracks occur that strongly depend on the applied load. The median, radial, and lateral cracks form the typical scratch pattern, while the lateral cracks can induce chipping by propagating towards the sample surface. Houérou et al. [38] summarize 3 different regimes in a schematic drawing (see **Figure 9)**, illustrating what can happen during a progressive scratch test: (I) in the micro-ductile regime, a permanent plastic track arises with possible sub-surface cracks underneath, (II) significant damage by surface cutting lateral cracks happens, and radial cracks characterize the so-called micro-cracking regime, (III) the micro-abrasive regime is characterized by a lot of debris and small lateral cracks.

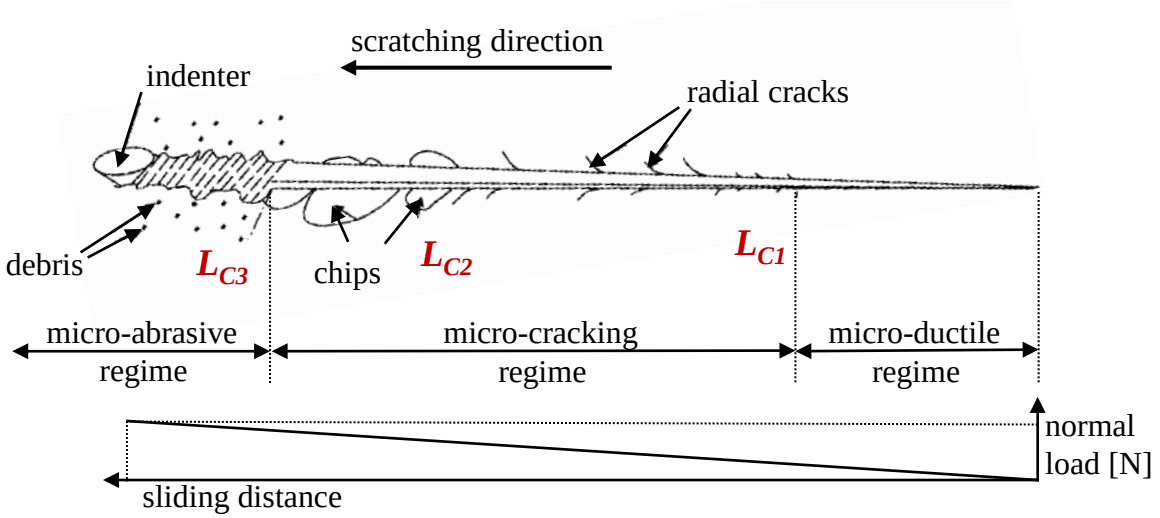

Figure 9: Typical scratch pattern on glasses during a progressive scratch with explanation of critical scratch loads, reprinted after [38].

According to Figure 9, the meaning of critical scratch loads can be explained and can be determined based on DIN EN ISO 1071-3 [43]. L_{C1}, as the first critical load appearing during scratching (Figure 9), is at the intersection of the first and the second regime, where the first radial cracks start to grow. If additionally chipping appears, it corresponds to L_{C2}. As soon as

the micro-abrasive regime is entered and debris particles are created along the scratch path, it is called L_{C3}.

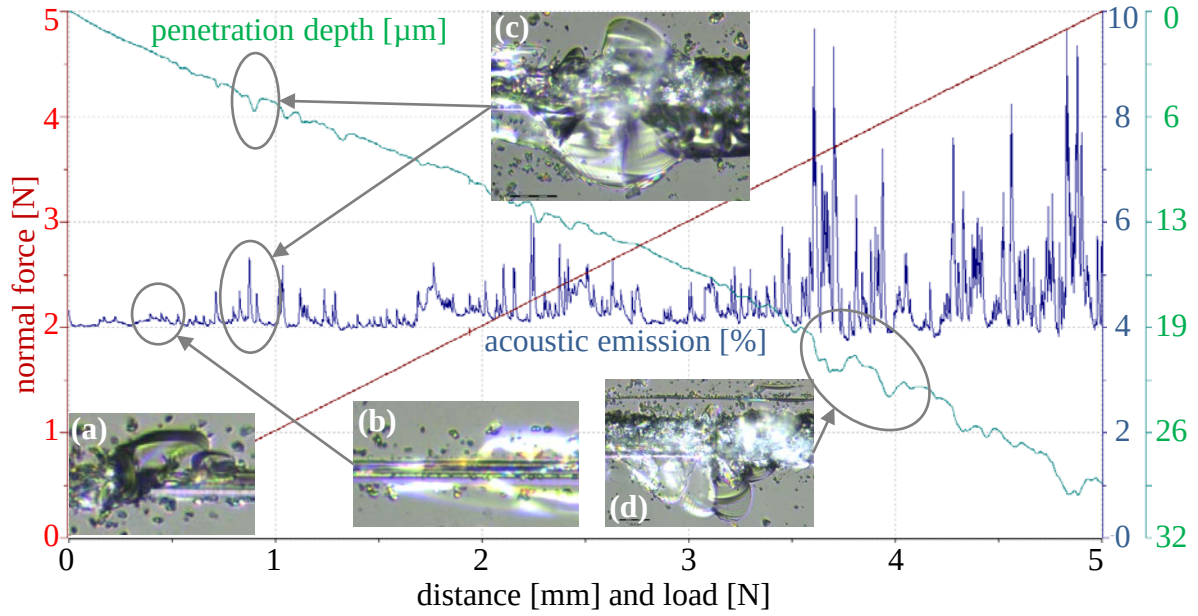

Figure 10: Example of scratch test record for N-BK7.

All scratches are produced with loads progressively increasing up to 5 N, while the system records the normal load, the penetration depth, and acoustic signals during the experiment. Afterwards the path is analyzed under an optical microscope so that the critical load values can be obtained by visual inspection. **Figure 10** illustrates an example of such a measurement with images inserted at certain points. Additionally, a graph of acoustic emission data obtained by the CSM integrate microphone and evaluated via the producers' software is given. The scratch starts with indenting the tip and then moving, which can lead to first damage (a). At the beginning, the acoustic emission is not clear enough so that in most cases the first critical load is not recognized and can only be obtained visually. But the first chipping and thus L_{C2} is recorded acoustically (b) and L_{C3} also causes a drop in the penetration depth (c). Picture (d) shows a big and noisy chipping area with a lot of debris and material removal with clear peaks. Herewith the critical scratch loads are measured and given for comparison in **Table 5**.

Table 5: Average critical scratch loads and corresponding penetration depths

Material	L_{C1} [N] (at penetration depth [µm])	L_{C2} [N] (at penetration depth [µm])	L_{C3} [N] (at penetration depth [µm])
Perlucor	0.35 ± 0.02 (at 2.1 ± 0.4)	0.53 ± 0.01 (at 3.1 ± 0.2)	1.43 ± 0.09 (at 7.2 ± 0.7)
NBK-7	0.35 ± 0.01 (at 1.7 ± 0.1)	0.55 ± 0.01 (at 3.2 ± 0.5)	0.71 ± 0.09 (at 3.7 ± 0.2)
Float glass	0.36 ± 0.01 (at 1.9 ± 0.2)	0.73 ± 0.02 (at 3.5 ± 0.4)	1.08 ± 0.03 (at 5.3 ± 1.1)
Float glass hardened	0.31 ± 0.04 (at 1.9 ± 0.4)	0.52 ± 0.09 (at 3.1 ± 0.3)	0.75 ± 0.01 (at 4.6 ± 0.8)
Borofloat	0.32 ± 0.01 (at 1.9 ± 0.5)	0.48 ± 0.01 (at 2.9 ± 0.3)	0.63 ± 0.02 (at 3.9 ± 0.5)
Borofloat hardened	0.28 ± 0.02 (at 1.6 ± 0.1)	0.43 ± 0.03 (at 2.4 ± 0.2)	0.58 ± 0.01 (at 3.9 ± 0.9)
Gorilla glass	0.3 ± 0.04 (at 1.9 ± 0.3)	0.61 ± 0.09 (at 3.7 ± 0.6)	1.14 ± 0.25 (at 6.6 ± 1)
Gorilla glass hardened	0.34 ± 0.03 (at 1.8 ± 0.2)	0.53 ± 0.07 (at 2.6 ± 0.5)	0.69 ± 0.01 (at 3.3 ± 0.3)
B270	0.33 ± 0.04 (at 1.8 ± 0.2)	0.69 ± 0.01 (at 3.4 ± 0.6)	1.28 ± 0.04 (at 6 ± 0.3)
B270 hardened	0.32 ± 0.06 (at 1.7 ± 0.4)	0.56 ± 0.06 (at 3 ± 0.5)	0.85 ± 0.04 (at 4.5 ± 1)

The polymer is not listed in Table 5, since it merely reveals an increasingly plastically deformed scratch without any cracks or regimes. All in all, the glasses behave mostly similar because crack initiation and propagation are unstable phenomena. So the values measured via the above mentioned method and the optical comparison could be helpful to classify the scratch resistance of the materials. In addition, the penetration depth of the sphero-conical indenter is given in the table.

In general, the hardened versions of the glasses reveal lower values for the critical scratch loads, because of their near-surface hardened layer that appears to be penetrated by the tip. As mentioned in the introduction, tempered glasses are often more sensitive to scratches [8]. The unhardened float glass and B270 show big chipping areas with high resulting damage; see **Figure 11**, presenting a representative scratch path for the different materials. The standard deviation in the table reveals that all materials behave fairly consistently. The only exception is

the unhardened Gorilla glass where an outlier was obtained, which is shown in the picture. Despite this outlier, the positive sandblasting resistance is not verified in scratch testing for both the unhardened and hardened Gorilla glasses. Except for Borofloat, all glasses display a great sensitivity for chipping. In the scratch experiments, unhardened B270 seems to be the most resistant glass. Again, unhardened N-BK7 arranges itself as an average glass; even hardened B270 and float glass have higher values for the critical load. Surprisingly, unhardened and hardened Borofloat reveal the worst scratch resistance, although the sandblasting resistance was not that bad. The spinel ceramic presents relatively constant behavior without forming big chips or cracks along the scratch path and, as such, shows the best scratch resistance with the highest L_{C3} values.

All three critical loads or regimes can be found in the range of less than 2 N. After that threshold, the scratch ground gets bigger and deeper with random chipping and crack formation along the path. Sub-surface lateral cracks can also be seen and usually remaining underneath the surface, e.g. for the unhardened float glass after the big black chip around 3 N. At this point, the chipping mechanism can be explained: because of attractive forces, two intersecting radial cracks on the same path side are connected through a lateral crack that reaches the surface of the sample and then leads to the removal of material in form of a chip.

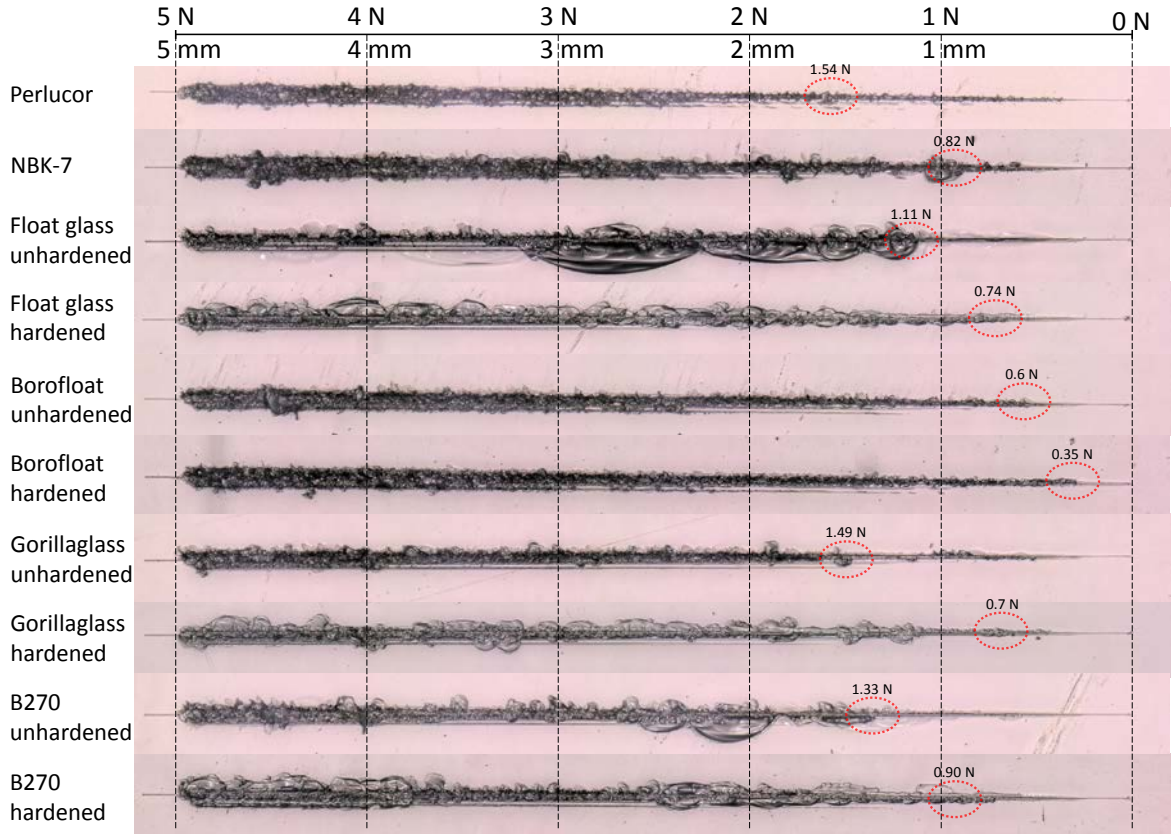

Figure 11: Exemplary scratch paths with load progressively increasing up to 5 N.

All in all, the scratch test results are not clearly distinguishable, and the correlation of the optical characterization with the other tests and with the mechanical properties is not significant. The meaning for the application-relevant consideration regarding wear and optical appearance is not clear, and hence scratch testing appears not to support or aid the interpretation of such results. Also, the values for the critical loads L_{C1} and L_{C2} are quite similar for all materials. At higher loads, the compressive surface layer of the hardened glasses is penetrated, which causes them to fail earlier than the unhardened ones with lower values for L_{C3}. This, in turn, makes them not really comparable to each other, to other test, and to mechanical parameters.

4. Conclusion

This research investigates the abrasion behavior and mechanical properties of transparent spinel ceramic and different glasses and assesses their behavior in case of chemical hardening by

comparing the two versions of each glass. Overall, when comparing the different materials, density and Poisson´s ratio are almost similar, and there does not appear to be a direct correlation with the other parameter or the effective abrasion resistance of the materials. Young´s moduli of all glasses are very similar and do not seem to affect the performance. Hardness is load-dependent, and the hardened glasses show a similar indentation size effect as the ceramic. Note, this research also reveals that a high level of hardness strongly influences the wear resistance of a material, especially in the case of short-term exposure. Except for Borofloat, fracture strength and toughness are in good agreement, and the fracture strength behavior is also reflected in the Weibull modulus. In addition, there appears to be a correlation between the hardness of the unhardened glasses measured at 100 mN and the fracture strength, but this is not really valid for the hardened ones.

Furthermore, the current work indicates that the fracture toughness is a very important parameter for the wear resistance, and high values promise a good long-term protection as indicated by the optical sandblasting results. The result goes along with a low mass loss and reduced roughness, except for the polymer which behaves quite elastically, consuming the impact energy of the sandblasting beam. High mass loss also results in a larger crater depth and agrees with lower hardness and fracture toughness values.

In the scratch experiments, all three predefined typical scratch damage regimes were observed and critical loads could be determined, however, the meaning of scratch tests regarding mechanical parameters, abrasion, and optical behavior after mechanical testing is unclear. The behavior of all critical scratch loads does not follow any other parameter, and there is no clear correlation. In fact, the differences in results seem to be mostly related to Young´s modulus and thus depend on the elastic deformation rather than on failure behavior, possibly a result of the rather large spherical tip used in this particular test.

Correlating with previous results, a ranking of general wear resistance of optical integrity could be introduced that appears to be most important for applications as a transparent protecting window:

The transparent spinel ceramic Perlucor exhibits by far the highest hardness with a high fracture toughness and resilience to sandblasting in terms of little mass loss. Indeed, it has the best wear resistance and the smallest optical changes, especially regarding the apparent transparency. Hardened Gorilla glass has the highest fracture strength and fracture toughness, as well as a very high value for the hardness. However, with respect to sandblasting exposure, it appears to be more prone to scratching damage and faster blurring than the ceramic material. The same applies to hardened Borofloat, which has very good mechanical values as well as resistance to sandblasting exposure, but has a poor scratch behavior. Hardened B270 displays the best scratch values of the hardened glasses and also quite high hardness and fracture strength, but poor performance during the sandblasting exposure with the highest mass loss. Hardened float glass resembles these results. N-BK7 can be considered an average glass. All in all, every unhardened glass behaves analogically with properties very close to each other. The polymer Polycarbonate is difficult to evaluate compared to the ceramic and glass materials because its high elasticity makes many tests unfeasible. As such, it demonstrates extremely fast blurring and the worst wear resistance with lowest hardness.

Acknowledgements

The research is founded under the European Union's research project Resistant Transparent Sensors (ResTraSe) EFRE-0800652 in the context of the regional development of NRW (EFRE.NRW). The authors are thankful for the support and all the samples provided by CeramTec-Etec GmbH, especially Ms. Helen Eschenauer as well as Dr. H. Marxer and acknowledge Ms. Tatjana Osipova of the Institute of Energy and Climate Research (IEK-2) for the technical support as well as Prof. L. Singheiser to enable this work.

References

[1] O. Tokariev, L. Schnetter, T. Beck, and J. Malzbender, "Grain size effect on the mechanical properties of transparent spinel ceramics," *Journal of the European Ceramic Society,* vol. 33, no. 4, pp. 749-757, 2013/04/01/ 2013.

[2] O. Tokariev, R. W. Steinbrech, L. Schnetter, and J. Malzbender, "Micro- and macro-mechanical testing of transparent MgAl2O4 spinel," *Journal of Materials Science,* journal article vol. 47, no. 12, pp. 4821-4826, June 01 2012.

[3] A. Krell, J. Klimke, and T. Hutzler, "Advanced spinel and sub-µm Al2O3 for transparent armour applications," *Journal of the European Ceramic Society,* vol. 29, no. 2, pp. 275-281, 2009/01/01/ 2009.

[4] M. Grujicic, W. C. Bell, and B. Pandurangan, "Design and material selection guidelines and strategies for transparent armor systems," *Materials & Design,* vol. 34, pp. 808-819, 2012.

[5] J. J. Swab *et al.*, "Determining the Strength of Coarse-Grained AlON and Spinel," *Journal of the American Ceramic Society,* vol. 97, no. 2, pp. 592-600, 2014.

[6] R. W. Tustison, *Window and dome technologies and materials XI: 15 - 16 April 2009, Orlando, Florida, United States* (Proceedings of SPIE, no. 7302). Bellingham, Wash.: SPIE, 2009, p. 390.

[7] D. B. Marshall and B. R. Lawn, "Residual stress effects in sharp contact cracking," *Journal of Materials Science,* journal article vol. 14, no. 8, pp. 2001-2012, August 01 1979.

[8] J. Schneider, S. Schula, and W. P. Weinhold, "Characterisation of the scratch resistance of annealed and tempered architectural glass," *Thin Solid Films,* vol. 520, no. 12, pp. 4190-4198, 2012.

[9] Bundesverband-Flachglas. (2003). *Reinigung von Glas; Merkblatt zur Glasreinigung*. Available: http://www.glas-bach.de/wp-content/uploads/2015/06/BF_Merkblatt_Glasreinigung.pdf

[10] T. Rogers, presented at the Proceedings of Glass Performance Days, 10th Conference, Tampere, Finland, 15–18.06.2007, 2007.

[11] A. B. Van Groenou, N. Maan, and J. Veldkamp, "Single-point scratches as a basis for understanding grinding and lapping," in *The Science of Ceramic Machining and Surface Finishing, NBS Special Publication 562,* vol. 2: US Government Printing Office Washington DC, 1979, pp. 43-60.

[12] K. Li, Y. Shapiro, and J. C. M. Li, "Scratch test of soda-lime glass," *Acta Materialia,* vol. 46, no. 15, pp. 5569–5578, 1998.

[13] S. J. Bull, "Failure modes in scratch adhesion testing," *Surface and Coatings Technology,* vol. 50, no. 1, pp. 25-32, 1991/01/01/ 1991.

[14] J. Malzbender and G. de With, "Scratch testing of hybrid coatings on float glass," *Surface and Coatings Technology,* vol. 135, no. 2, pp. 202-207, 2001/01/15/ 2001.

[15] A. Krell, T. Hutzler, and J. Klimke, "Transmission physics and consequences for materials selection, manufacturing, and applications," *Journal of the European Ceramic Society,* vol. 29, no. 2, pp. 207-221, 2009/01/01/ 2009.

[16] K. C. Datsiou and M. Overend, "Artificial ageing of glass with sand abrasion," *Construction and Building Materials,* vol. 142, pp. 536-551, 2017.

[17] N. Adjouadi, N. Laouar, C. Bousbaa, N. Bouaouadja, and G. Fantozzi, "Study of light scattering on a soda lime glass eroded by sandblasting," *Journal of the European Ceramic Society,* vol. 27, no. 10, pp. 3221-3229, 2007/01/01/ 2007.

[18] C. Bousbaa, A. Madjoubi, M. Hamidouche, and N. Bouaouadja, "Effect of annealing and chemical strengthening on soda lime glass erosion wear by sand blasting," *Journal of the European Ceramic Society,* vol. 23, no. 2, pp. 331-343, 2003/02/01/ 2003.

[19] S. Bouzid and N. Bouaouadja, "Effect of impact angle on glass surfaces eroded by sand blasting," *Journal of the European Ceramic Society,* vol. 20, no. 4, pp. 481-488, 2000/04/01/ 2000.

[20] A. J. Sparks and I. M. Hutchings, "Transitions in the erosive wear behaviour of a glass ceramic," *Wear,* vol. 149, no. 1, pp. 99-110, 1991/09/30/ 1991.

[21] CeramTec, "Materialkenndaten Perlucor," 2017.

[22] Corning. (2016). *Corning Gorilla Glass 5 Data Sheet*. Available: https://www.corning.com/microsites/csm/gorillaglass/PI_Sheets/Corning%20Gorilla%20Glass%205%20PI%20Sheet.pdf
[23] EUROGLAS. (2014). *Datenblatt Floatglas*. Available: https://www.glastroesch.de/fileadmin/user_upload/EUROGLAS_Produkte_und_Daten.pdf
[24] Kümpel. (2018). *Datenblatt Polycarbonat*. Available: https://www.kuempel.com/fileadmin/PDFs/Datenblaetter_und_Zertifikate/PC_Technisch.pdf
[25] Schott, "Datenblatt N-BK7," ed, 2017.
[26] U. OPTICS. (2018). *Data Sheet Schott B270 Superwite*. Available: https://www.uqgoptics.com/pdf/Schott%20B270.pdf
[27] U. OPTICS. (2018). *Data Sheet Schott Borofloat*. Available: https://psec.uchicago.edu/Papers/Schott_Borofloat.pdf
[28] A. Standard, "ASTM E 1876-01: Standard Test Method for Dynamic Youngs Modulus, Shear Modulus, and Poissons Ratio by Impulse Excitation of Vibration," *Annual Book of ASTM Standards, ASTM, West Conshohocken, PA*, 2015.
[29] J. Malzbender, "Comment on hardness definitions," *Journal of the European Ceramic Society*, vol. 23, no. 9, pp. 1355-1359, 2003.
[30] D. Norm, "EN ISO 14577-1 Instrumentierte Eindringprüfung zur Bestimmung der Härte und anderer Werkstoffparameter–Teil 1 Prüfverfahren," ed: DIN, 2003.
[31] W. C. Oliver and G. M. Pharr, "An improved technique for determining hardness and elastic modulus using load and displacement sensing indentation experiments," *Journal of Materials Research*, vol. 7, no. 6, pp. 1564-1583, 1992.
[32] G. R. Anstis, P. Chantikul, B. R. Lawn, and D. B. Marshall, "A Critical-Evaluation of Indentation Techniques for Measuring Fracture-Toughness .1. Direct Crack Measurements," (in English), *Journal of the American Ceramic Society*, vol. 64, no. 9, pp. 533-538, 1981.
[33] A. G. Evans and T. R. Wilshaw, "Quasi-static solid particle damage in brittle solids—I. Observations analysis and implications," *Acta Metallurgica*, vol. 24, no. 10, pp. 939-956, 1976/10/01/ 1976.
[34] A. Standard, "C1499–05: Standard test method for monotonic equibiaxial flexural strength of advanced ceramics at ambient temperature," *Annual Book of ASTM Standards, ASTM, West Conshohocken, PA*, 2003.
[35] J. Malzbender, R. Steinbrech, and L. Singheiser, "Failure probability of solid oxide fuel cells," in *Ceramic engineering and science proceedings*, 2009, vol. 26, pp. 293-298.
[36] E. DIN, "843-5: 2007-03:„Hochleistungskeramik-Mechanische Eigenschaften monolithischer Keramik bei Raumtemperatur-Teil 5: Statistische Auswertung “," *Deutsche Fassung EN*, pp. 843-5, 2006.
[37] https://www.mhg-strahlanlagen.de/de/strahlanlagen/strahlmittel/glaskugeln.html. (2018). *Data Sheet MHG glass beads Typ 207*.
[38] V. Le Houérou, J. C. Sangleboeuf, S. Dériano, T. Rouxel, and G. Duisit, "Surface damage of soda–lime–silica glasses: indentation scratch behavior," *Journal of Non-Crystalline Solids*, vol. 316, no. 1, pp. 54-63, 2003/02/01/ 2003.
[39] T. Li, K. Visvanathan, and Y. B. Gianchandani, "A batch-mode micromachining process for spherical structures," *Journal of Micromechanics and Microengineering*, vol. 24, no. 2, 2014.
[40] M. Buijs and K. K.-v. Houten, "Three-body abrasion of brittle materials as studied by lapping," *Wear*, vol. 166, no. 2, pp. 237–245, 1993.
[41] A. A. Wereszczak and C. E. Anderson, "Borofloat and Starphire Float Glasses: A Comparison," *International Journal of Applied Glass Science*, vol. 5, no. 4, pp. 334-344, 2014.
[42] O. Tokariev, *Micro- and macro- mechanical testing of transparent MgAl2O4 spinel* (Schriften des Forschungszentrums Jülich Reihe Energie & Umwelt, no. 215). p. 99.
[43] K. Taube, "Qualitätssicherung an tribologischen Schichten – Eigenschaften und Meßverfahren," *Materialwissenschaft und Werkstofftechnik*, vol. 31, no. 7, pp. 616-624, 2000.